Loughborough University

This item was submitted to Loughborough's Research Repository by the author.
Items in Figshare are protected by copyright, with all rights reserved, unless otherwise indicated.

An automotive engine charge-air intake conditioner system: analysis of fuel economy benefits in a gasoline engine application

PLEASE CITE THE PUBLISHED VERSION

PUBLISHER

Professional Engineering Publishing / © IMECHE

VERSION

VoR (Version of Record)

LICENCE

CC BY-NC-ND 4.0

REPOSITORY RECORD

Taitt, D.W., Colin P. Garner, E. Swain, D. Blundell, R.J. Pearson, and J.W.G. Turner. 2019. “An Automotive Engine Charge-air Intake Conditioner System: Analysis of Fuel Economy Benefits in a Gasoline Engine Application”. figshare. https://hdl.handle.net/2134/4830.

Loughborough University

This item was submitted to Loughborough's Institutional Repository (https://dspace.lboro.ac.uk/) by the author and is made available under the following Creative Commons Licence conditions.

creative commons

COMMONS DEED

Attribution-NonCommercial-NoDerivs 2.5

You are free:

- to copy, distribute, display, and perform the work

Under the following conditions:

Attribution. You must attribute the work in the manner specified by the author or licensor.

Noncommercial. You may not use this work for commercial purposes.

No Derivative Works. You may not alter, transform, or build upon this work.

- For any reuse or distribution, you must make clear to others the license terms of this work.
- Any of these conditions can be waived if you get permission from the copyright holder.

Your fair use and other rights are in no way affected by the above.

This is a human-readable summary of the Legal Code (the full license).

Disclaimer

For the full text of this licence, please go to:
http://creativecommons.org/licenses/by-nc-nd/2.5/

An automotive engine charge-air intake conditioner system: analysis of fuel economy benefits in a gasoline engine application

D W Taitt[1], **C P Garner**[1], **E Swain**[1]*, **D Blundell**[2], **R J Pearson**[2], and **J W G Turner**[2]
[1]Wolfson School of Mechanical and Manufacturing Engineering, University of Loughborough, Loughborough, Leicestershire, UK
[2]Group Lotus plc, Norwich, UK

The manuscript was received on 16 May 2005 and was accepted after revision for publication on 2 May 2006.

DOI: 10.1243/09544070JAUTO94

Abstract: A combination of analytical techniques has been used to quantify the potential fuel economy benefits of an automotive engine charge-air intake conditioner system applied to a spark-ignited gasoline engine. This system employs a compressor, intercooler, and expander to provide increased charge density with the possibility of reducing charge-air temperature below sink temperature. This reduction in charge-air temperature provides the potential for improved knock resistance at full load; thereby allowing the possibility of increasing compression ratio with corresponding benefits in thermodynamic cycle efficiency and part-load fuel economy. The four linked and interfaced models comprised a first-law thermodynamic model of the charge-air conditioner system, a one-dimensional engine cycle simulation, a two-zone combustion model, and a knock criterion model. An analysis was carried out under full load at 3000 r/min and showed that a charge-air conditioner system – with compressor, intercooler, and expander efficiencies of 0.8 – allowed the compression ratio to be increased by approximately half a ratio, which gave up to 1.5 per cent reduction in brake specific fuel consumption at 2000 r/min 2 bar brake mean effective pressure when compared with a conventional pressure charger intercooler system with no expander.

Keywords: internal combustion engine, pressure charging, intercooling, charge-air temperature, expander, compression ratio, knock, fuel economy

1 INTRODUCTION

This paper is the second in a series addressing the subject of an automotive charge-air intake conditioner system that seeks to increase charge air density in spark ignition (SI) gasoline engines by expansion cooling. A summary of the main issues discussed in the first paper [**1**] includes here, for completeness, some background to the research, the operating principles of expansion cooling and the key results and conclusions from the first paper.

This paper then goes on to describe a new piece of work which uniquely integrates four analytical models to arrive at a quantitative analysis of the potential fuel economy benefits of the system. This includes:

(a) enhancement of the existing first-law thermodynamic model to characterize system performance at constant net power output;
(b) engine cycle simulation performance modelling;
(c) two-zone combustion modelling;
(d) knock modelling.

1.1 Fuel economy, downsizing, and pressure charging

Fuel economy continues to be one of the most important drivers of engine technology; with the combination of engine downsizing and intake pressure charging being particularly applicable to throttled SI engines.

* *Corresponding author: Wolfson School of Mechanical and Manufacturing Engineering, University of Loughborough, Loughborough, Leicestershire, LE11 3TU, UK. email: E.Swain@Lboro.ac.uk*

The full fuel economy benefits of this approach are, however, rarely realized since the full load requirement for knock-free combustion (with pressure charging) demands that the engine compression ratio be reduced, with a corresponding loss of thermodynamic efficiency and a consequent increase in fuel consumption. Although variable compression ratio mechanisms can be used to address this issue they are necessarily complex and present significant challenges in terms of reliability, weight, and cost.

An alternative approach involves finding a way of achieving knock-free full-load combustion while maintaining a high (fixed) compression ratio. Intercooling is widely employed to reduce the propensity for knock to occur by using a process of irreversible heat transfer to lower charge-air temperature. With such a system, however, it is not possible to reduce charge-air temperature below the sink temperature.

1.2 Charge-air intake conditioner system

The charge-air conditioner system proposed by Turner *et al.* [**2**] and shown in schematic form in Fig. 1, uses an exhaust turbine driven compressor and an intercooler. However, it differs from a conventional system by using a screw expander to expand the intake air after the intercooler to achieve a further reduction in temperature and pressure along with a corresponding recovery of work through a mechanical link to the crankshaft.

1.3 Previous work

The work described in this paper is the continuation of an earlier piece of work [**1**] in which a first-law thermodynamic model was developed and used to characterize the performance of an automotive charge-air intake conditioner system. Because this stand-alone analysis did not include an engine model it was necessarily carried out at constant charge-air density and mass flowrate. It did, however, yield the important conclusion that a charge-air intake conditioner system was capable of delivering reductions in charge-air temperature and that its performance was dependent upon intercooler effectiveness, expander isentropic efficiency, and compressor isentropic efficiency, in order of decreasing sensitivity.

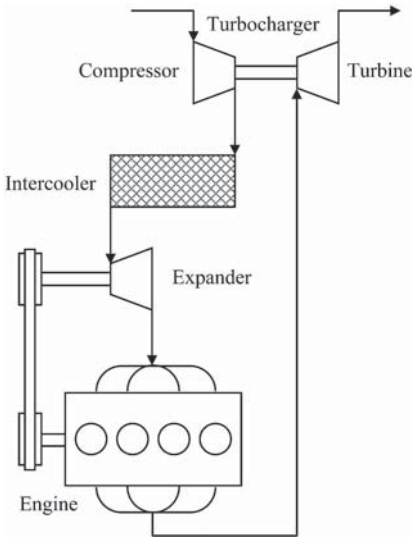

Fig. 1 Charge-air intake conditioner system as proposed by Turner *et al.* [**2**]

1.4 Objective

The objective of this new research was to quantify the potential fuel economy benefits of an automotive charge-air intake conditioner system at the steady state part-load mapping point of 2000 r/min 2 bar brake mean effective pressure (BMEP).

2 CONSTANT NET POWER FIRST-LAW MODEL

This work was an essential precursor to the main fuel economy analysis; comprising the necessary modifications and enhancements to the first-law thermodynamic model, described in the first paper of the series [**1**], to allow it to interface with the engine cycle simulation code and also to provide an early indication of the viability of the system.

2.1 Modified first-law model

The system proposed by Turner *et al.* [**2**] and shown in Fig. 1 is a particular case of a charge-air intake conditioner system using a turbine-driven compressor and a belt drive from the expander to the engine crankshaft. The first-law model used here was rather more generic; simply recognizing that the compressor required a power input and the expander delivered a power output. The configuration shown schematically in Fig. 2 had a relatively simple interface with the engine. This required just one interfacing boundary condition (the net power required to drive the charge-air intake conditioner system) and greatly simplified the modelling process.

The first-law model (shown schematically in Fig. 2) was modified with the addition of a simple engine air flow model which quantified the relationship between engine brake power, charge air density, and mass flowrate. This model was based on gasoline SI engine full-load performance being a strong function of air mass flowrate such that, for a given engine and a given speed, brake-specific air consumption

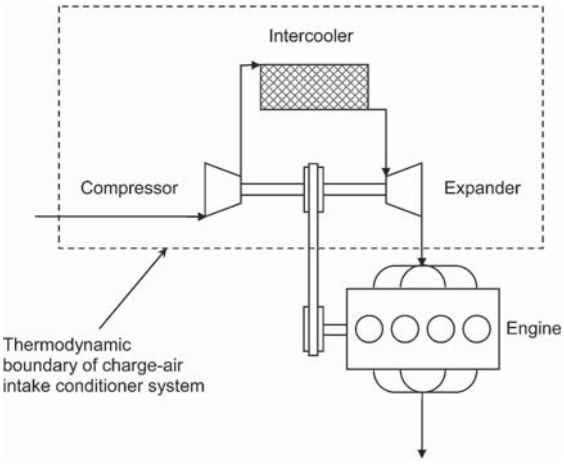

Fig. 2 Simplified charge-air intake conditioner system as modelled thermodynamically

(BSAC) did not vary greatly and could be taken as constant.

The simplified engine air flow model is described as follows. Charge-air mass flowrate, $\dot{m}$, is given by

$$\dot{m} = P_{\text{brake}}\text{BSAC} \tag{1}$$

where P_{brake} is engine brake power. The charge-air volume flowrate, $\dot{V}$, is a function of engine swept volume, V_{d}, engine rotational speed, N, the number of crank revolutions per power stroke, n, and volumetric efficiency (based on inlet plenum conditions), η_{v}, giving

$$\dot{V} = \eta_{\text{v}} V_{\text{d}} \frac{N}{n} \tag{2}$$

Charge-air inlet density, ρ, is defined

$$\rho = \frac{\dot{m}}{\dot{V}} \tag{3}$$

Thus, substituting equations (1) and (2) into equation (3) gives

$$\rho = \frac{nP_{\text{brake}}}{V_{\text{d}} N \eta_{\text{v}}}\text{BSAC} \tag{4}$$

Having modified the first-law model to interface with the engine cycle simulation code a brief analysis was performed to confirm that the system maintained its effectiveness under conditions of constant net power.

2.2 Constant net power analysis

When considering the effectiveness of the system, it is important to differentiate between charge-air temperature as an absolute value and charge-air temperature reduction as a function of the performance of the charge-air intake conditioner system performance. Accordingly, a system performance parameter T_{rel} is defined as charge air temperature relative to that at an expander pressure ratio $r_{\text{ex}} = 1.0$ (equivalent to a conventional pressure-charged and intercooled engine with no expander).

The model was used to map the system performance parameter T_{rel} across a range of compressor isentropic efficiency, intercooler effectiveness, and expander isentropic efficiency values, details of which are given in Table 1 along with the constants used in the analysis. Figure 3(a) shows the performance sensitivity of the system at 190 kW net power. The results show that the system was capable of delivering reductions in charge-air temperature at constant net power output and that its performance remained more sensitive to the isentropic efficiency of the expander than to that of the compressor. For typical compressor and expander efficiencies (0.7 and 0.5) the system performance delivered T_{rel} values in the range 0 to -5 K. A limited sensitivity analysis was carried out to identify whether system performance could be improved by reducing the net power requirement and increasing intercooler effectiveness.

Figure 3(b) shows system performance sensitivity at a net power requirement of 157 kW. Comparing with Fig. 3(a) shows that the system performance parameter T_{rel} was improved by a factor of 2 (approximately). From Fig. 3(c) it can be seen that system performance was a strong function of intercooler effectiveness and that an increase from 0.8 to 0.9 resulted in an improvement in T_{rel} by a further factor of 2 (approximately).

3 FUEL ECONOMY ANALYSIS

The objective of this research was to determine the potential fuel economy benefits of a charge-air intake conditioner system as applied to a gasoline SI

Table 1 Study variables and constants – constant net power analysis

Parameter	Value
Study variables	
Compressor isentropic efficiency, η_{comp}	0.6–0.8
Expander isentropic efficiency, η_{ex}	0.4–0.8
Intercooler effectiveness, E_{IC}	0.6–0.9
Net engine brake power, P_{net}	190 kW, 157 kW
Constants	
Engine speed, N	6000 r/min
Brake specific air consumption, BSAC	4.0 kg/kW h
Volumetric efficiency, η_{v}	0.95
Ambient air temperature, T_{atm}	302 K
Ambient air pressure, p_{atm}	1.013×10^5 Pa

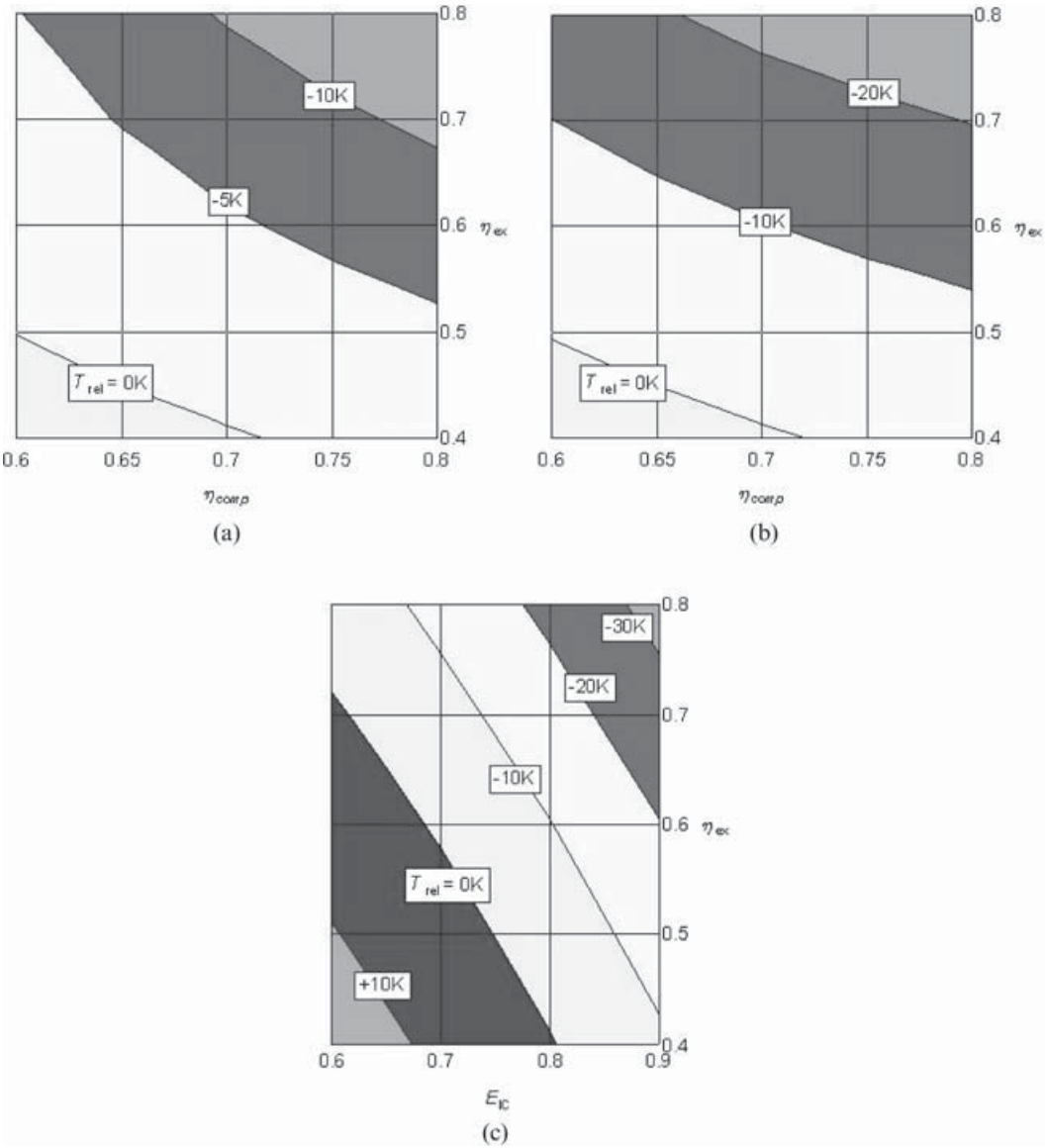

Fig. 3 System performance sensitivity: (a) $P_{net} = 190$ kW, $r_{comp} = 4.0$, $E_{IC} = 0.8$; (b) $P_{net} = 157$ kW, $r_{comp} = 4.0$, $E_{IC} = 0.8$; (c) $P_{net} = 157$ kW, $r_{comp} = 4.0$, $\eta_{comp} = 0.7$

engine. This involved linking four analytical models to determine the relationship between charge-air temperature, trapped charge temperature, knock resistance, compression ratio, and part-load fuel economy. The subject of the research described in this paper was the Lotus NOMAD engine (Fig. 4), details of which have been published by Turner *et al.* [**3**]. The research described in this paper was closely aligned with the Lotus NOMAD project and indeed used experimental results to validate the analysis.

The charge-air conditioner system used on the NOMAD engine was as shown schematically in Fig. 1: comprising a turbine-driven compressor, a water-cooled intercooler, and a twin-screw expander, with poly-vee belt drive back to the engine crankshaft.

3.1 Analytical approach

In order to determine the fuel economy benefit of the system it was necessary to understand and quantify the relationship between charge-air temperature, trapped charge temperature, knock limit, and compression ratio. This was accomplished by using four linked analytical models (Fig. 5). The first-law thermodynamic model was used to determine the properties of the charge-air at the outlet of the expander. These properties were then used as inlet boundary conditions for the engine cycle simulation which was run to determine the in-cylinder trapped conditions of the charge which, in turn, were used as boundary conditions for the two-zone combustion

Fig. 4 Lotus NOMAD experimental engine

model. From this, the end-gas temperature and pressure histories could be determined and then used, in integral form, in a knock criteria function to determine knock limit.

3.1.1 Performance parameters

The analytical approach was based on the recognition that fuel economy is a direct function of compression ratio and that, up to a point, fuel economy improves with increasing compression ratio. This simplified the analysis, with the main focus being the application and control of the charge-air conditioner system to attain the maximum possible compression ratio for a given net power output requirement. This critical compression ratio could then be used to determine the part-load fuel economy.

3.1.2 Study variables

The study involved mapping maximum net power as a function of compressor and expander pressure ratio and also as a function of engine compression ratio. From the mapped data it would be possible to determine the maximum attainable compression ratio for a given net power output. The study variables are listed in Table 2, which also details the range of values used in the study.

3.1.3 Control variables

At each analysis point, defined by the study variables of compression ratio and compressor and expander pressure ratio, the phasing of the combustion event was varied to determine the maximum net power. The two-zone combustion model and knock criteria model were employed to establish the critical combustion phase angle at which knock occurred. While Fig. 6 shows typically how torque varies with ignition angle it should be noted that peak cylinder pressure and exhaust gas temperature may also impose operating limits that prevent the use of the optimum combustion phasing.

3.1.4 Constants

The propensity for knock to occur is a function of, among other factors, cylinder end-gas temperature and pressure [**4**]. These properties increase with load and typically attain their highest values around the maximum point on the BMEP curve. From this it could be concluded that, for a fixed compression ratio engine, the critical knock limit would occur around the maximum brake torque point and, for the NOMAD engine, this was taken as 3000 r/min.

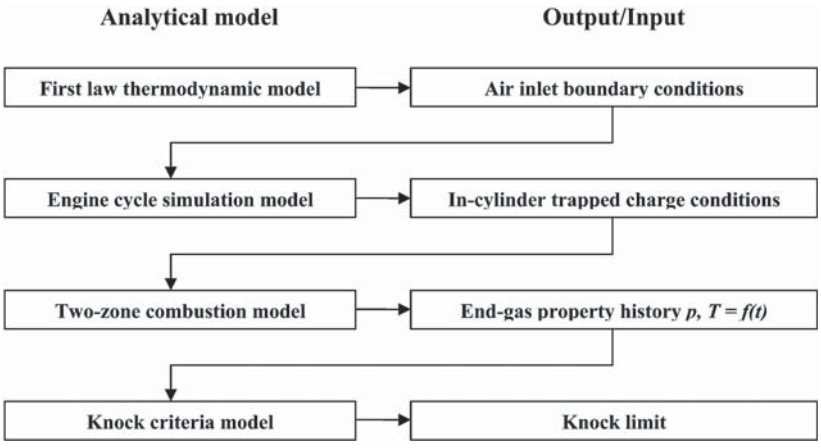

Fig. 5 Analytical approach: four linked models

Table 2 Study variables and constants – fuel economy analysis

Parameter	Value
Study variables	
Compression ratio, r_c	6 : 1, 8 : 1, 9 : 1, and 10 : 1
Compressor pressure ratio, r_{comp}	1.5, 2.0, 2.5, 3.0, 3.5, and 4.0
Expander pressure ratio, r_{ex}	1.0, 1.2, 1.5, 2.0, and 2.5
Constants	
Compressor isentropic efficiency, η_{comp}	0.8
Expander isentropic efficiency, η_{ex}	0.8
Intercooler effectiveness, E_{IC}	0.8
Engine speed, N	3000 r/min
Ambient air temperature, T_{atm}	302 K
Ambient air pressure, p_{atm}	1.013×10^5 Pa
Equivalence ratio, ϕ	1.1
Fuel octane number	97.3 RON

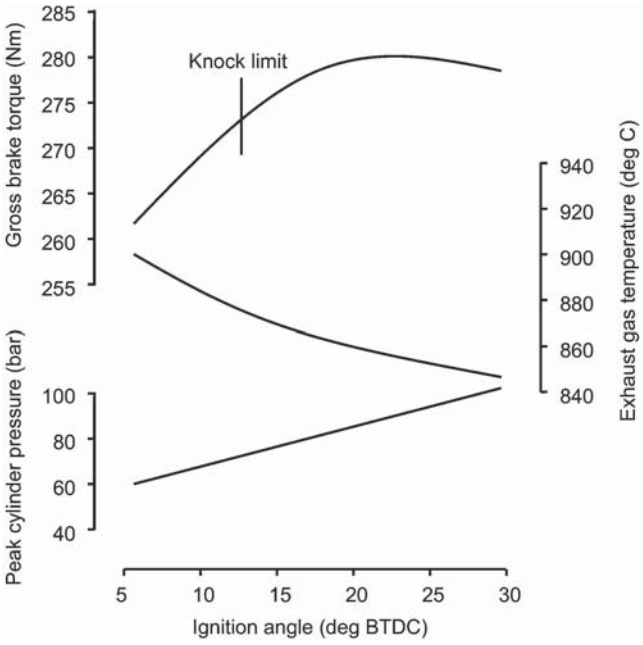

Fig. 6 Typical example of knock-limited combustion at 3000 r/min full load

Given that the objective of this piece of work involved determining the relationship between reduced charge-air inlet temperature and engine fuel economy, it was necessary that the specified efficiency of the charge-air conditioner system should be high enough, within practical limits, to deliver a significant reduction in charge-air temperature. In recognition of these factors a constant value of 0.8 was used for compressor and expander isentropic efficiency and for intercooler effectiveness; lower values failing to give any significant reduction in charge-air inlet temperature and higher values being unrealistic for practical automotive compressors intercoolers and expanders.

Atmospheric temperature and pressure were held constant at 302 K ($\sim$25 °C) and 1.013 bar, respectively. A fuel research octane number (RON) of 97.3 was used and a fuel : air equivalence ratio, ϕ, of 1.1 was used throughout the analysis, where ϕ is defined by

$$\phi = \frac{\text{actual fuel : air mass ratio}}{\text{stoichiometric fuel : air mass ratio}} \quad (5)$$

The constants used in the fuel economy analysis are detailed in Table 2.

3.2 First-law thermodynamic model

3.2.1 Charge-air conditioner system

The engine and charge-air conditioner system were modelled as shown schematically in Fig. 2. This allowed the engine itself to be modelled as pseudo naturally aspirated, with intake boundary conditions matched to the charge-air properties at the expander outlet.

Each analysis point was defined by the compressor and expander pressure ratios and the first-law model was used to determine the properties of the charge-air at the expander outlet and the power input requirement of the charge-air intake conditioner system. Charge-air mass flowrate in the first-law thermodynamic model was matched to that of the engine cycle simulation.

3.3 Engine cycle simulation

3.3.1 Description of model and operating principles

The analysis used Lotus Engine Simulation (LES). This is a one-dimensional engine performance cycle simulation code. The closed-period model uses a single-zone heat release approach while the manifold gas dynamics are based on the one-dimensional equations of compressible fluid flow in ducts [**5**, **6**]. The resulting governing equations of flow in the manifolds are solved, in conservation law form, using

the two-step Lax–Wendroff finite difference scheme and a symmetric total variation diminishing flux limiter.

3.3.2 *Application*

LES is a commercially available code and has been used and validated across a wide range of engines and operating conditions. In this analysis it was used to determine engine brake power and in-cylinder trapped charge conditions (at the inlet valve closing point); the single-zone combustion model of LES precluding the determination of knock limit. The engine cycle simulation code was also used to determine cylinder head, piston crown, and cylinder liner temperatures which were required inputs for the two-zone combustion model.

The defining features of the NOMAD engine and the main parameters used in the LES input file are detailed below in Table 3. A schematic of the model is shown in Fig. 7. The LES model was pseudo naturally aspirated and used modified inlet and exhaust boundary conditions to model a pressure charged engine. The inlet boundary conditions were matched to the expander outlet while the minimum cross-sectional area of an exhaust outlet throttle was calibrated to match measured pre-turbine exhaust back pressure. The LES model did not include a compressor and expander because this would have provided no incremental accuracy or validity to the analysis. It would however have complicated the correlation of the LES model with a number of additional variables.

Of particular note is the unusual valve timing resulting in very little overlap (1.5°). This timing was used on the NOMAD engine to avoid the high residual exhaust gas fraction in the intake charge normally associated with high pre-turbine exhaust back pressure and thus high exhaust–inlet pressure differential.

Table 3 NOMAD engine specification

Feature	Value
Bore	82.5 mm
Stroke	79.5 mm
Compression ratio	10.34 : 1
Inlet valve opening (IVO)	0.5° ATDC
Inlet valve closing (IVC)	65.5° ABDC
Exhaust valve opening (EVO)	48° BBDC
Exhaust valve closing (EVC)	2° ATDC
Inlet–exhaust overlap	1.5°
Target maximum power	190 kW at 6000 r/min

ATDC, after top dead centre; ABDC, after bottom dead centre; BBDC, before bottom dead centre.

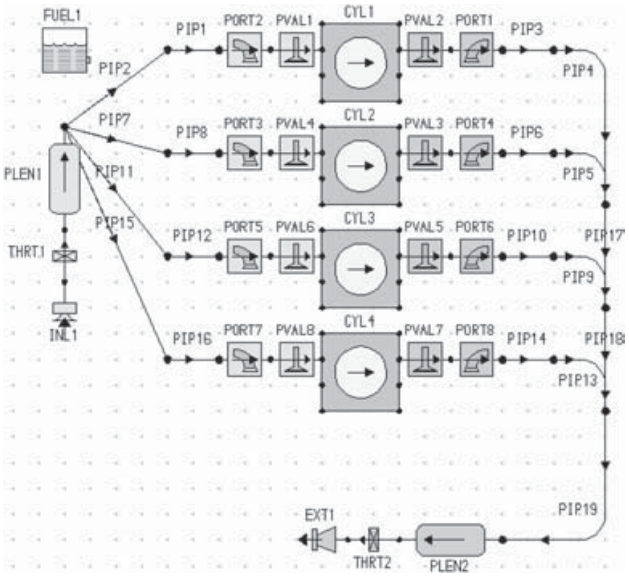

Fig. 7 Engine cycle simulation – schematic model

3.3.3 *Validation*

The LES code incorporated variable heat transfer and heat release coefficients which could, if required, be used to calibrate the model. For this analysis the default values, shown below in Table 4, proved to be satisfactory and no changes were made to these coefficients.

The engine cycle simulation model was validated against experimental test results from the NOMAD engine at a 3000 r/min full-load condition. Table 5 shows the correlation of these results while Fig. 8 shows cylinder pressure as a function of crank angle for the analytical model and the experimental engine. Generally the model correlated very well against the experimental test results; the crank angle resolved cylinder pressure results being particularly good. The model gave a brake torque output of 252 N m, compared with a measured result of 262 N m. This correlation error was considered acceptable at less than 5 per cent, given the possibility of test measurement error and use of the default friction model [**7**] in the cycle simulation code. There was little analytical value in tuning the friction model to reduce this

Table 4 Engine cycle simulation – heat transfer and heat release coefficients

Model	Coefficient	Value
Heat transfer (open cycle); Annand	A	0.2
	B	0.8
Heat transfer (closed cycle); Annand	A	0.12
	B	0.8
	C	4.29×10^{-9}
Combustion; Wiebe	A	10
	M	2

Table 5 Engine cycle simulation – correlation against experimental measurements

Parameter	Units	Measured value	Modelled value
Speed	r/min	3000	3000
Brake torque	N m	262	252
BSFC	g/kW h	270	269
Charge air temperature	°C	34.5	34.0
Charge air pressure (absolute)	bar	2.19	2.19
Exhaust temperature	°C	975	984
Exhaust pressure (absolute)	bar	1.75	1.75
Equivalence ratio	—	1.1	1.1
Ignition angle	° BTDC	6	6
Peak cylinder pressure	bar	60	60

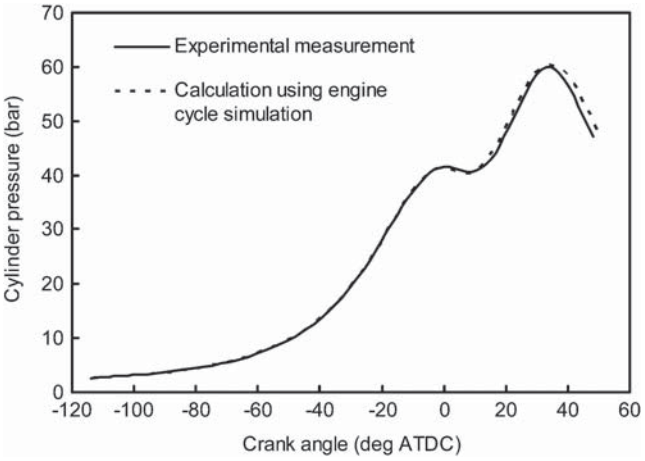

Fig. 8 Combustion correlation at 3000 r/min full load – engine cycle simulation model

discrepancy since the study was to address comparative rather than absolute values. Accordingly, the default friction model was retained.

3.4 Two-zone combustion model

3.4.1 Description of model and operating principles

The cycle simulation code was used to supply initial boundary conditions for a more sophisticated two-zone 'flame propagation' model, similar to that described by Horlock and Winterbone [**8**], in which a spherical flame front demarcates the burned and unburned gases. The turbulent flame speed U_t is defined as

$$U_t = U_l F_t \tag{6}$$

where U_l is the laminar flame speed and F_t is the turbulent flame speed factor.

Heat transfer to the engine components is calculated using Annand's equation [**9**] with cylinder head, piston crown, and cylinder liner wall being treated as separate areas for heat transfer and having different surface temperatures. The combustion model is based on equilibrium thermodynamics and considers the reaction of a general hydrocarbon fuel in air, giving 13 product species. Seven equilibrium reactions are considered and a 7-equation model for the rate controlled formation of nitric oxide is used [**10**]. The model was used to determine the time-resolved temperature and pressure histories of the unburned gas region so that a knock criterion could be applied.

3.4.2 Validation

The model was calibrated to match the crank angle resolved cylinder pressure measurements from the NOMAD engine. The default Annand heat transfer coefficients ($A = 0.2$ and $B = 0.8$ with radiation being neglected) were retained for the two-zone combustion model while a value of 4.5 was used for the turbulent flame speed factor, F_t.

The model was validated against measured cylinder pressure results from the NOMAD engine as shown in Fig. 9. It was not possible to validate end-gas temperatures since no measured results were available. While the general shape of the modelled

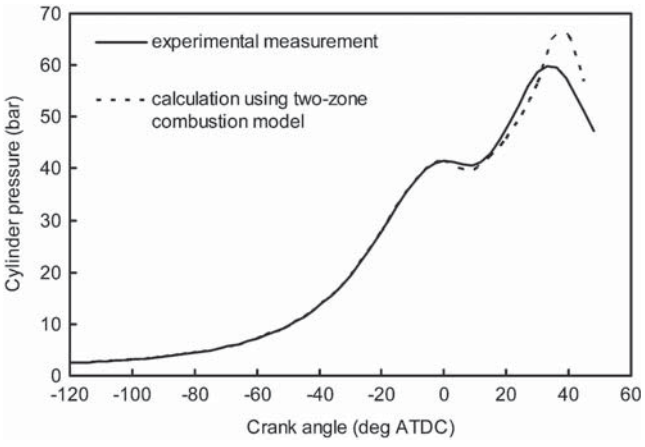

Fig. 9 Combustion correlation at 3000 r/min full load – two-zone combustion model

cylinder pressure characteristic followed that of the measured results the model over-predicted the peak cylinder pressure and it was not possible to tune the turbulent flame speed factor or ignition delay period to improve the match. A possible contributing factor to this discrepancy was the inability of the two-zone combustion model to accommodate the effects of charge motion and mixture stratification. Despite this, the correlation error was accepted on the basis that these results would not be used to directly determine an absolute value of a performance parameter, such as the brake output of the engine, but rather they would be used in an empirical knock criterion model which would itself be subject to calibration and validation. It was however recognized that future work would benefit from the application of a more advanced multi-zone combustion model.

3.5 Knock model

3.5.1 Description of model and operating principles

The knock model used was of a type based on an empirical induction time correlation, derived by matching an Arrhenius function to measured data on induction or auto-ignition times for given air–fuel mixtures over relevant pressure and temperature ranges [**11**]. It is then assumed that auto-ignition occurs when

$$\int_{t=0}^{t} \frac{\mathrm{d}t}{\tau} = 1 \tag{7}$$

where τ is the induction time at the instantaneous temperature and pressure for the mixture, t is the elapsed time from the start of the end-gas compression process ($t = 0$).

A number of empirical expressions for induction time have been developed [**12**] which have the form

$$\tau = Ap^{-n} \exp\left(\frac{B}{T}\right) \tag{8}$$

where A, n, and B are coefficients that depend upon the fuel.

The most extensively tested correlation, proposed by Douaud and Eyzat [**4**] and based on work by Livengood and Wu [**13**], was used for this analysis:

$$\tau = 17.68\left(\frac{\mathrm{RON}}{100}\right)^{3.402} p^{-1.7} \exp\left(\frac{3800}{T}\right) \tag{9}$$

where τ is in milliseconds, p is absolute pressure in atmospheres, T is temperature in Kelvin, and RON is the fuel octane number.

Substituting equation (9) into equation (7) gives an expression that defines the onset of auto-ignition when

$$\int_{t=0}^{t} \frac{\mathrm{d}t}{17.68\left(\frac{\mathrm{RON}}{100}\right)^{3.401} p^{-1.7} \exp\left(\frac{3800}{T}\right)} = 1 \tag{10}$$

3.5.2 Application

The analysis used a numerical integration (trapezoid rule) of the time-resolved end-gas temperature and pressure histories with data points at 1° crank angle intervals from which the value of $\int_{t=0}^{t} \mathrm{d}t/\tau$ at the end of combustion was compared against the critical integral value of 1.0.

3.5.3 Validation

The knock model was validated against measured results at the 3000 r/min combustion correlation point for which the knock-limited ignition point had been established by experiment at 6° BTDC. The engine cycle simulation and two-zone combustion models were run for a range of ignition angles between 0° and 12° BTDC at 2° increments and the end-gas temperature and pressure histories were analysed using the knock model to determine the critical knock limit. Figure 10 shows the plots of $\int_{t=0}^{t} \mathrm{d}t/\tau$ versus t for each of the ignition angles. It is clear that the critical knock-limited ignition angle was between 6° and 8° BTDC and correlated well with the measured test result from the NOMAD engine.

Having successfully interfaced and validated the four component analytical tools the composite model was then used to conduct a parametric study. This quantified the beneficial effects of reduced charge-air temperature on knock limit, compression ratio, and fuel economy through the use of a charge-air intake conditioner system. The results of this piece of work are presented in the following section.

3.6 Results

3.6.1 Effect of compression ratio

Figure 11 shows the relationship between net power and compressor pressure ratio at a fixed expander pressure ratio of 1.0. This is equivalent to a conventional pressure charged and intercooled engine with no expander. The family of curves shows the effect of increasing compression ratio (from 6 : 1 to 10 : 1) at constant expander pressure ratio of 1.0. At low compressor pressure ratios the curves show net power increasing almost linearly with compressor pressure ratio with power being a strong function

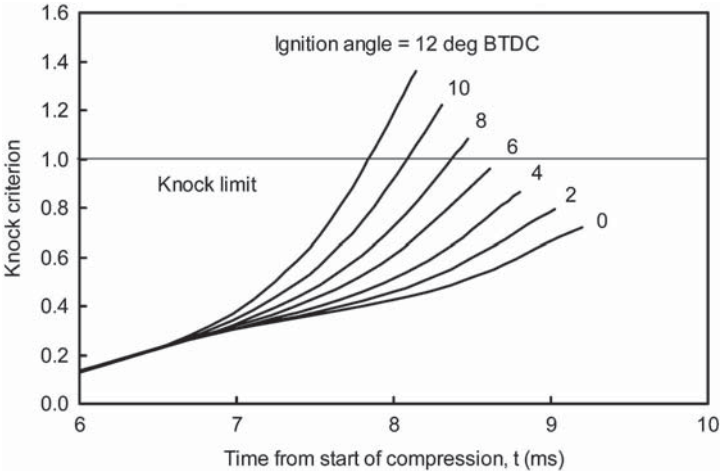

Fig. 10 Knock model correlation at 3000 r/min full load

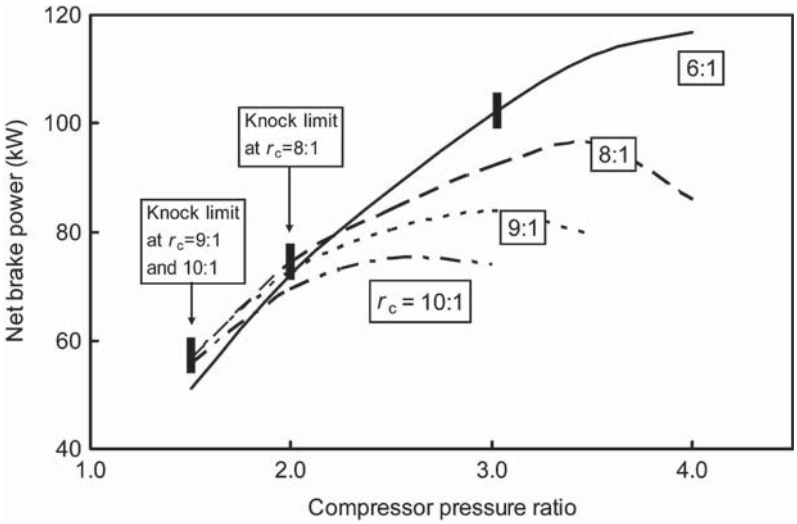

Fig. 11 Effect of compression ratio, r_c, on knock-limited net brake power at 3000 r/min full load ($r_{ex} = 1.0$)

of charge-air mass flowrate. At these relatively low compressor pressure ratios, and in cases where combustion was not knock-limited, net brake power was higher at increased compression ratio. This was consistent with the definition of the thermodynamic efficiency of the ideal constant volume cycle by which cycle efficiency increases with compression ratio

$$\eta = 1 - \frac{1}{r_c^{\gamma - 1}} \tag{11}$$

where r_c is the compression ratio and γ is the ratio of specific heats for the working fluid.

At higher compressor pressure ratios the gradient of the curves reduced as the combustion became knock-limited, with the effect that higher compression ratios experienced a greater degree of knock-limit and accordingly required retarded combustion phasing giving correspondingly lower net power output. (It should be noted that the onset of knock-limited combustion was marked by the point at which the gradient of the curve started to reduce rather than the point at which it became zero.) These results were entirely consistent with the well-known requirement for reducing compression ratio with increased pressure charging on SI gasoline engines and provided a measure of confidence in the analytical method.

3.6.2 *Effect of expander pressure ratio*

Figure 12(a) also plots net power against compressor pressure ratio but in this case the family of curves shows the effect of increasing expander pressure

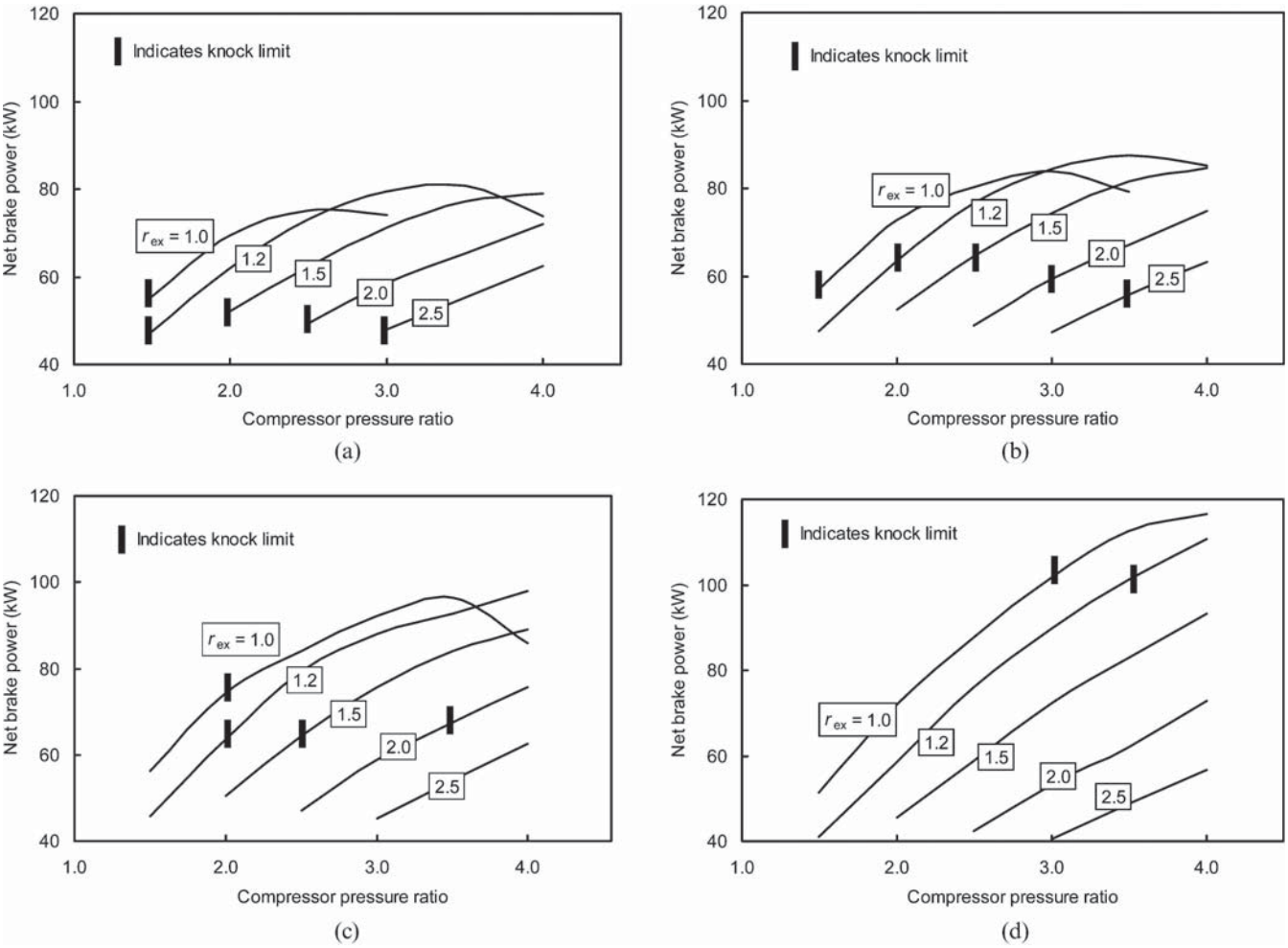

Fig. 12 Effect of expander pressure ratio, r_{ex}, on knock-limited net brake power at 3000 r/min full load. Compression ratio, r_c: (a) 10 : 1; (b) 9 : 1; (c) 8 : 1; (d) 6 : 1

ratio (from 1.0 to 2.5) at a constant compression ratio of 10 : 1. Generally, for a given net power requirement, a higher expander pressure ratio requires a correspondingly higher compressor pressure ratio in order to deliver the required charge density and air mass flowrate. It is, however, apparent that the maximum net power output of 81 kW for an expander pressure ratio of 1.2 exceeds the corresponding maximum value of 75 kW for an expander pressure ratio of 1.0. This is a particularly important result as it demonstrates that, for a given compression ratio, an engine using a charge-air intake conditioner system may be capable of delivering better performance than an equivalent engine using conventional pressure charging and intercooling.

Figures 12(b), (c), and (d) show the results of similar analyses at compression ratios of 9 : 1, 8 : 1, and 6 : 1, respectively. It can be seen that at 9 : 1 and 8 : 1 compression ratio, as with 10 : 1, maximum net power increased with expander pressure ratio. Although it was unclear from any of these analyses whether or indeed where this characteristic might have achieved a maximum value, two practical operating limits were applied. Firstly it was felt unreasonable to expect a typical automotive charge-air compressor to maintain an isentropic efficiency of 0.8 beyond $r_{comp} = 4.0$ and secondly an exhaust gas temperature limit of 950 °C was imposed in recognition of the requirement for the integrity and durability of the exhaust manifold.

Within these constraints, and for the specific conditions of this analysis, it was apparent that, at 10 : 1 compression ratio, a charge-air conditioner system operating with an expander pressure ratio of 1.2 could offer a net power improvement of approximately 6.5 per cent over a conventional pressure-charging and intercooling system with no expander. From this it could be inferred that a net power output of 75 kW, in this instance, could be achieved at a higher compression ratio using a charge-air intake

conditioner system running at an expander pressure ratio of 1.2. Figures 12(a), (b), and (c) were analysed to quantify the extent to which compression ratio could be increased by the application of a charge-air intake conditioner system running with an expander pressure ratio of 1.2.

Figure 12(c) shows a maximum net power of 96 kW for $r_{ex} = 1.0$ and 101 kW for $r_{ex} = 1.2$ at a compression ratio of 8 : 1. Figure 12(b) shows maximum net power of 88 kW for $r_{ex} = 1.2$ at 9 : 1 compression ratio. Linear interpolation was used (between 101 kW at 8 : 1 and 88 kW at 9 : 1) to determine that for a maximum net power requirement of 96 kW a charge-air intake conditioner system running with an expander pressure ratio of 1.2 could be used to increase compression ratio from 8.0 : 1 to 8.4 : 1.

A similar analysis of Figs 12(a) and (b) leads to the result that for a maximum net power requirement of 84 kW a charge-air intake conditioner system running with an expander pressure ratio of 1.2 will allow compression ratio to be increased from 9.0 : 1 to approximately 9.6 : 1 (based on linear interpolation between 88 kW at 9 : 1 and 81 kW at 10 : 1).

3.6.3 *Part-load fuel economy*

The engine cycle simulation model was used to determine part-load BSFC at 2000 r/min 2 bar BMEP as a function of compression ratio. Figure 13 shows the characteristic curve of reducing BSFC with increasing compression ratio from which the fuel economy benefits at 96 kW and 84 kW were derived at 1 and 1.5 per cent, respectively. In this final analysis the fuel economy benefits of the system, although quantifiable, were nevertheless very small and a brief study was conducted to identify the possible reasons for this and the limiting factors.

3.6.4 *Charge-air temperature and trapped charge temperature*

In the course of the fuel economy analysis it became apparent that while the charge-air intake conditioner system was capable of delivering charge air at low temperatures the corresponding trapped charge temperatures were significantly higher. Figure 14 is an example of a typical result showing the variation of charge-air inlet temperature and trapped charge temperature as the compressor pressure ratio was increased from 2.0 to 4.0 (while, in this case, the expander pressure ratio and compression ratio were held fixed at 1.5 and 10 : 1, respectively).

Clearly the beneficial effect of the charge-air conditioner system was greatly reduced by the increase in charge-air temperature between the expander outlet and the cylinder. While it is certainly the case that heat transfer from the throttle, intake manifold, inlet port, cylinder head, and cylinder walls would have contributed in part to the increase in charge temperature, a further factor was the effect of the residual exhaust gas trapped in the cylinder with the fresh charge.

In section 3.3.2 it was explained that the valve timing of the NOMAD engine was specified with very little overlap (1.5°) in order to minimize the trapped mass of residual exhaust gas. This was necessary on the experimental engine because of the high pre-turbine exhaust pressure and the correspondingly high adverse pressure differential between the intake and exhaust ports. A hypothesis was proposed that a mechanically driven compressor may be more suitable than an exhaust turbine driven device because the exhaust system would be significantly less restrictive and so would present the possibility of a beneficial pressure differential between the

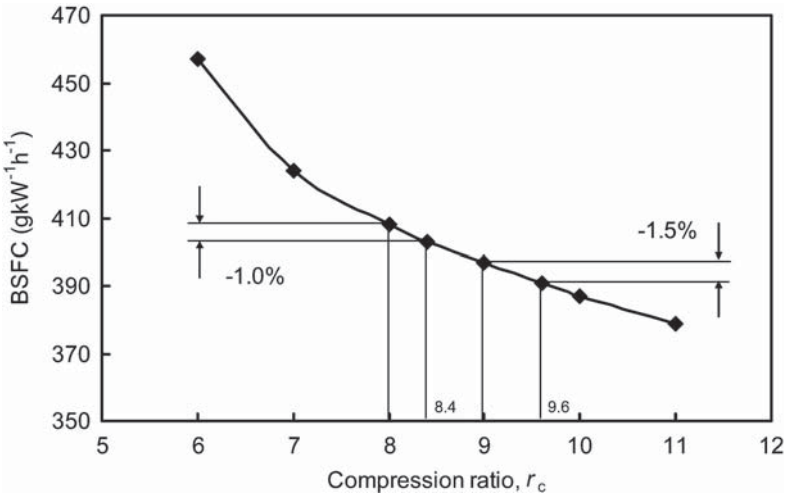

Fig. 13 Effect of compression ratio, r_c, on BSFC at 2000 r/min 2 bar BMEP

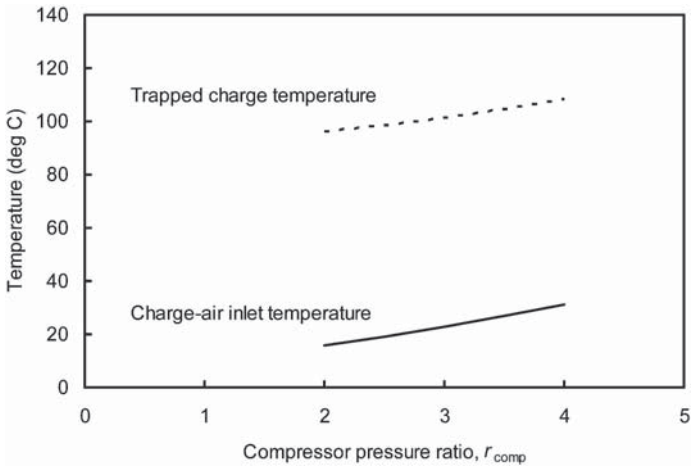

Fig. 14 Relationship between charge-air inlet temperature and trapped charge temperature at 3000 r/min full load. Compression ratio, $r_c = 10:1$, expander pressure ratio, $r_{ex} = 1.5$

intake and exhaust ports. In this hypothetical case it would be possible to exploit valve timing with significant overlap in order to use the intake–exhaust pressure differential to purge the cylinder of residual exhaust gases during the overlap period and so reduce the temperature of the trapped charge.

Further investigation on this subject was beyond the scope of this piece of research but was considered worthy of a future study; particularly in the areas of reducing heat transfer from the engine to the charge and also in reducing the trapped mass of residual exhaust gases.

4 CONCLUSIONS

1. Four analytical models were successfully interfaced, validated, and applied in order to quantify the potential fuel economy benefits of an automotive charge-air intake conditioner system. The four models are summarized below:
   (a) first-law thermodynamic model of a charge-air intake conditioner system;
   (b) one-dimensional engine cycle simulation;
   (c) two-zone combustion model;
   (d) knock criteria model.
2. The first-law thermodynamic model was enhanced with the inclusion of a simple engine airflow model. This was used in a preliminary analysis to confirm that the charge-air intake conditioner system maintained its effectiveness under conditions of constant engine net brake power output. The model was also used to perform a limited sensitivity analysis which showed that the ability of the system to reduce charge-air temperature could be significantly improved by increasing intercooler effectiveness and reducing the engine net brake power requirement. The opportunity to reduce engine net brake power is however limited since it conflicts with the broader objective of using high specific output to achieve improved fuel economy through aggressive engine downsizing.
3. The Lotus NOMAD experimental engine was modelled using a charge-air intake conditioner system with compressor, intercooler, and expander efficiencies of 0.8. The analysis showed that for a given compression ratio, and for a limited range of conditions, the charge-air intake conditioner could be used to increase maximum net power by up to 6.5 per cent. Alternatively, for a given maximum net power requirement, the charge-air intake conditioner system could be used to achieve an increase in compression ratio of approximately half a ratio and this resulted in a reduction in BSFC at 2000 r/min 2 bar BMEP of approximately 1.5 per cent.
4. Although the fuel economy improvements in this particular case were small, it became apparent that the full beneficial effect of the charge-air conditioner system was not realized as a result of the significant increase in charge-air temperature (approximately 80 °C) between the expander outlet and the cylinder. This was attributable, in part at least, to heat transfer from the engine and trapped residual exhaust gases.
5. The research described in this paper has established the theoretical feasibility of an automotive charge-air intake conditioner in SI gasoline engine applications for increased net power or reduced BSFC. While the full-load performance benefit of the system was significant at 6.5 per cent, the BSFC reduction of 1.5 per cent was of marginal

benefit, although there may yet be merit in further work to lower the trapped charge temperature. This may be achieved through the reduction of heat transfer from the engine and also by the use of mechanical supercharging and valve overlap to exploit the beneficial inlet–exhaust pressure differential to scavenge the cylinder of residual exhaust gases.

ACKNOWLEDGEMENTS

The authors wish to thank the Royal Academy of Engineering and Perkins Engines for their financial support of the second author. They also thank Group Lotus plc for supplying the NOMAD engine test data used for this work.

REFERENCES

1 **Taitt, D. W., Garner, C. P., Swain, E., Bassett, M. D., Pearson, R. J.,** and **Turner, J. W. G.** An automotive engine charge-air intake conditioner system: thermodynamic analysis of performance characteristics. *Proc. Instn Mech. Engrs, Part D: J. Automobile Engineering*, 2005, **219**(D3), 389–404.

2 **Turner, J. W. G., Pearson, R. J., Bassett, M. D.,** and **Oscarsson, J.** Performance and fuel economy enhancement of pressure charged SI engines through turbo expansion – an initial study. SAE paper 2003-01-0401, 2003.

3 **Turner, J. W. G., Pearson, R. J., Bassett, M. D., Blundell, D. W.,** and **Taitt, D. W.** The turboexpansion concept – initial dynamometer results. SAE paper 2005-01-1853, 2005.

4 **Douaud, A. M.** and **Eyzat, P.** Four-octane-number method for predicting the anti-knock behaviour of fuels and engines. SAE paper 780080, 1978.

5 **Winterbone, D. E.** and **Pearson, R. J.** *Design techniques for engine manifolds*, 1999 (Professional Engineering Publications, London).

6 **Winterbone, D. E.** and **Pearson, R. J.** *Theory of engine manifold design*, 2000 (Professional Engineering Publications, London).

7 **Barnes-Moss, H. W.** A designer's viewpoint. In Proceedings of IMechE Conference on *Passenger Car Engines*, 1975, pp. 133–147 (MEP, London).

8 **Horlock, J. H.** and **Winterbone, D. E.** *The thermodynamics and gas dynamics of internal combustion engines*, vol. 2, 1986 (Clarendon Press, Oxford).

9 **Annand, W. J. D.** Heat transfer in the cylinder of reciprocating internal combustion engines. *Proc. Instn Mech. Engrs*, 1963, **177**, 973–990.

10 **Baruah, P. C.** Combustion and cycle calculations in spark ignition engines. In *The thermodynamics and gas dynamics of internal combustion engines*, vol. 2 (Eds. J. H. Horlock and D. E. Winterbone), 1986, Ch. 14 (Clarendon Press, Oxford).

11 **Heywood, J. B.** *Internal combustion engine fundamentals*, 1988 (McGraw-Hill, New York).

12 **By, A., Kempinski, B.,** and **Rife, J. M.** Knock in spark ignition engines. SAE paper 810147, 1981.

13 **Livengood, J. C.** and **Wu, P. C.** Correlation of autoignition phenomenon in internal combustion engines and rapid compression machines. In Proceedings of Fifth International Symposium on *Combustion*, Pittsburgh, Pennsylvania, 1955, p. 347.

APPENDIX

Notation

A	coefficient
ABDC	after bottom dead centre
ATDC	after top dead centre
B	coefficient
BBDC	before bottom dead centre
BTDC	before top dead centre
BMEP	brake mean effective pressure (Pa)
BSAC	brake specific air consumption (kg/kW h)
BSFC	brake specific fuel consumption (g/kW h)
C	coefficient
E	intercooler effectiveness
F	flame speed factor
m	mass (kg)
M	coefficient
n	number of crank revolutions per power stroke, exponent
N	engine rotational speed (r/s)
p	pressure (Pa)
P	power (kW)
r	ratio
RON	research octane number
s	specific entropy (J/kg K)
SI	spark ignition
T	temperature (K)
U	flame speed (m/s)
V	volume (m^3)
γ	ratio of specific heats
η	efficiency
ρ	density (kg/m^3)
τ	induction time (ms)
ϕ	equivalence ratio

Subscripts

atm	atmospheric
brake	brake
c	compression
comp	compressor pressure

d	engine displacement
ex	expander pressure
IC	intercooler
l	laminar
net	net
rel	relative to condition at $r_{ex} = 1.0$
sys	system
t	turbulent
v	volumetric

Superscripts

$\dot{}$	derivative with respect to time (s^{-1})
$'$	ideal process